Heliyon 5 (2019) e03061

Contents lists available at ScienceDirect

Heliyon

journal homepage: www.cell.com/heliyon

Research article

Chirality discrimination at the carvone air/liquid interfaces detected by heterodyne-detected sum frequency generation

Yang Wang [a], Jianbin Du [a], Xiangyun Ma [a], Huijie Wang [a], Keng C. Chou [b], Qifeng Li [a,*]

[a] School of Precision Instrument and Opto-electronics Engineering, Tianjin University, Tianjin, China
[b] Department of Chemistry, University of British Columbia, Vancouver, BC, V6T 1Z1, Canada

ARTICLE INFO

Keywords:
Analytical chemistry
Organic chemistry
Physical chemistry
Enantiomers
HD-SFG
Air/liquid interface
Intrinsic chirality

ABSTRACT

The chiral signal of the carvone air/liquid interface is probed by heterodyne-detected sum frequency generation (HD-SFG) without the electronic resonance. The chiral SFG spectra exhibit two distinguishable spectral signatures. Four chiral vibrational peaks of the R- and S-carvone molecules are with opposite signs, which can directly determine the surface molecular chirality. Two achiral vibrational peaks are also observed with the same sign. The different spectral signatures can provide a detailed chirality characterization at the molecular interface.

1. Introduction

With the increasing demand of the chemical and pharmaceutical industries, molecular chirality at interfaces has attracted more and more attention in recent year [1,2]. Probing the chirality at interface is still a challenge to chiroptical techniques. Several linear optics and spectroscopic techniques, such as circular dichroism (CD), optical rotation dispersion (ORD), and Raman optical activity (ROA) have been used to study the molecular chirality in the bulk, but not at the interfaces [3, 4, 5]. The nonlinear spectroscopy including second harmonic generation (SHG) and sum frequency generation (SFG) have shown the ability to detect the chirality from the thin film or a monolayer [6,7].

Chiral vibrational SFG has become a power tool for detecting chiroptical activity [8, 9, 10, 11, 12, 13, 14, 15, 16, 17, 18]. Chiral SFG was first experimentally demonstrated by Shen's group to probe the bulk chiral liquid [8]. Chiral vibrational SFG is intrinsically suitable for chirality characterization at interfaces, owing to its interface, chiral and vibrational selectivity [10,13,17,19, 20, 21]. In particular, heterodyne-detected SFG (HD-SFG) [22, 23, 24] can be used to discriminate enantiomers at interfaces because of its phase sensitivity [13,14,16].

Comparing with the biomolecules, the chirality characterization of small molecules at interfaces are still rarely studied in the laboratory. Monoterpenes, such as limonene and carvone, are a class of important small molecules, which have antitumor, antimicrobial and antioxidant activities [25,26]. They are also an important component in air pollution [27]. Some characteristics of monoterpenes are most likely related to the interactions and signal transductions at the interface, for example, their enantiomers always have distinguishable odors [28,29]. Limonene molecules at the air/liquid have been studied as a benchmark molecule [12,13].

In this work, we report the chiral spectra of the carvone molecules at their air/liquid interfaces using phase sensitive HD-SFG. Carvone liquid has lower vapour pressure than limonene liquid, which can keep a stable air/liquid interface position among the HD-SFG measurement. The chiral spectra of the S-carvone and R-carvone molecules in the C–H stretching vibration region show two types of distinguishable features, which indicates the chiral and achiral spectral features respectively. The phase resolved chiral spectra can be used to directly distinguish between enantiomers at the carvone air/liquid interface.

2. Materials and methods

2.1. Sample preparation

S- and R-carvone were purchased from Sigma-Aldrich. The racemic mixture of carvone were prepare with a 1:1 ratio of S- and R-carvone. Three glass culture dishes (5 mm deep and 60 mm in diameter) were cleaned by a mixture of concentrated sulfuric acid (70%) and H_2O_2 (30%) for 2 h. The solution was filled into the dish with a depth of 3 mm.

* Corresponding author.
E-mail address: qfli@tju.edu.cn (Q. Li).

https://doi.org/10.1016/j.heliyon.2019.e03061
Received 14 November 2018; Received in revised form 23 March 2019; Accepted 12 December 2019

All samples and containers were freshly prepared just before the experiment.

2.2. The HD-SFG setup

The detailed HD-SFG setup has been described previously [30,31]. Briefly, a picosecond 800 nm beam and a femtosecond IR beam were temporally and spatially overlapped on the sample with incident angles of 50° and 60°, respectively. The SFG, 800 nm, and IR beams reflected from the sample were refocused on a GaAs wafer. The SFG from the sample was time-delayed by passing through a silica window with a thickness of 1 mm. The interference spectrum between the SFG from the sample was recorded by a charge-coupled device (CCD) camera after through a polarizer, a band-pass filter and a monochromator. The interference spectra of samples were normalized against that of a quartz crystal to obtain the phase-sensitive imaginary part, Im ($\chi^{(2)}$), spectra of $\chi^{(2)}$. We acquired the SFG spectra of the S-carvone, R-carvone, and the racemic mixture at air/liquid interfaces with SSP and PSP polarization combinations.

3. Results and discussion

In our HD-SFG Setup, a correction for the reflection coefficient of the IR beam should be needed [32]. The reflectivity of carvone liquid has varied complex components in the C–H stretching vibration region because of its vibrational resonance. The correction mainly is based on the frequency dependent complex index of refraction of carvone liquid [33]. All of Im ($\chi^{(2)}$) spectra of the carvone air/liquid interfaces are presented by correction.

Figure 1 shows the Im ($\chi^{(2)}$) spectra of the S-, R- and the racemic mixture of carvone at the air/liquid interface with SSP polarization combination. The Im ($\chi^{(2)}$) spectra are similar, confirming that these spectral features are originated from the achiral spectral response. The spectra show highly congested features in the C–H stretching region from 2800 cm^{-1} to 3000 cm^{-1}. There are two apparent achiral vibrational peaks at frequencies 2923 cm^{-1} and 2988 cm^{-1}. The signs of the spectra are all negative, indicating that the corresponding functional groups of the S- and R-carvone have the same orientation. According the polarization selection rule [34], the negative sign also indicates that the strong vibrational peaks in the SSP spectra most likely belong to the symmetric CH_3/CH_2 stretching modes and Fermi resonance modes.

Figure 2 shows the Im ($\chi^{(2)}$) spectra of the S-, R- and the racemic mixture of carvone at the air/liquid interface with PSP polarization combination, which is chiral-sensitive. Compared with the achiral signals, the chiral signals are almost 3 orders of magnitude weaker and show significantly different spectral features. In our work, the visible beam is at 800 nm, which is far from the electronic-resonance of carvone. Owing to the high sensitive of HD-SFG, the chiral spectra with a high signal-to-noise ratio has been recorded despite the fact that it is difficult to detect the chiral signal of small molecules in the reflection geometry [9,12,13].

As shown in Figure 2, the chiral spectra show two types of distinguishable features with several clear vibrational peaks. To determine the peak positions accurately, the PSP spectra are fitted by

$$\mathrm{Im}(\chi^{(2)}) = \sum \frac{A_q}{(\omega - \omega_q) + i\Gamma_q} \quad (1)$$

where A_q, ω_q and Γ_q are the amplitude, frequency, and linewidth of the q^{th} vibrational mode. The fitting results are listed in Table 1 and the fitted peak frequency are labelled with vertical dashed lines in Figure 2. Firstly, vibrational peaks at 2821 cm^{-1}, 2873 cm^{-1}, 2910 cm^{-1} and 2957 cm^{-1} have opposite signs in the spectra of S- and R-carvone. Secondly, vibrational peaks at 2932 cm^{-1} and 2992 cm^{-1} have the same sign in the spectra of S-, R- and the racemic mixture of carvone.

In the PSP Im ($\chi^{(2)}$) spectra, four clear vibrational peaks, labelled with purple vertical dashed lines in Figure 2, have opposite signs at the same frequencies for S- and R-carvone enantiomers, while these peaks in the racemic mixture spectrum are nearly cancelled. The opposite signs can directly identify the opposite handedness of each enantiomers. We have demonstrated the ability of HD-SFG to directly probe the chirality at interfaces even without the electronic-resonance. The three strong vibrational peaks can be assigned to symmetric CH_2 (2821 cm^{-1}), symmetric CH_3 (2873 cm^{-1}) and single CH (2910 cm^{-1}) stretching modes respectively [8,35]. The weak vibrational peak at 2957 cm^{-1} likely belongs to the asymmetric CH_2 or CH_3 stretching mode, because it has the opposite sign to the symmetric stretching peaks at 2821 cm^{-1} and 2873 cm^{-1}.

The chiral PSP Im ($\chi^{(2)}$) spectra of S- and R-carvone in Figure 2 are not exactly mirror images of each other, though the chiral SFG signal of enantiomers might have only opposite phases to each other. In fact, the non-resonant backgrounds play a role to break the imaging symmetry. In our work, all the chiral spectra are shifted up from the zero line with a small positive non-resonant backgrounds. However, the amplitude value of each chiral vibrational peak is still almost same.

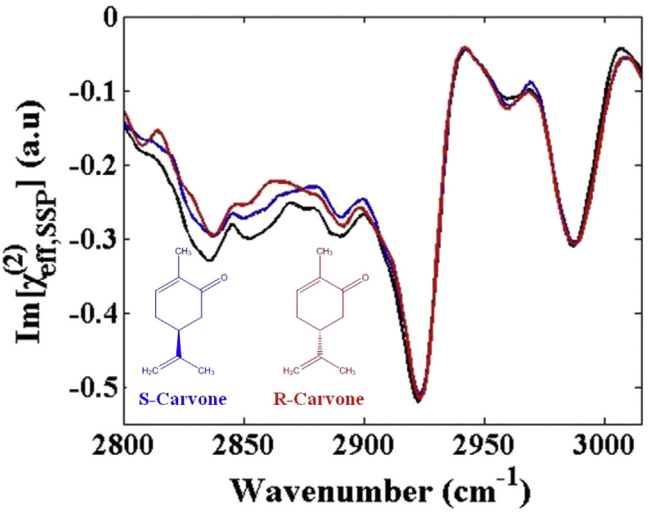

Figure 1. The Im ($\chi^{(2)}$) spectra of the carvone air/liquid interfaces with SSP polarization combination: S-carvone (blue), R-carvone (red), racemic mixture (black). The subgraph is the molecular structures of S- and R-carvone.

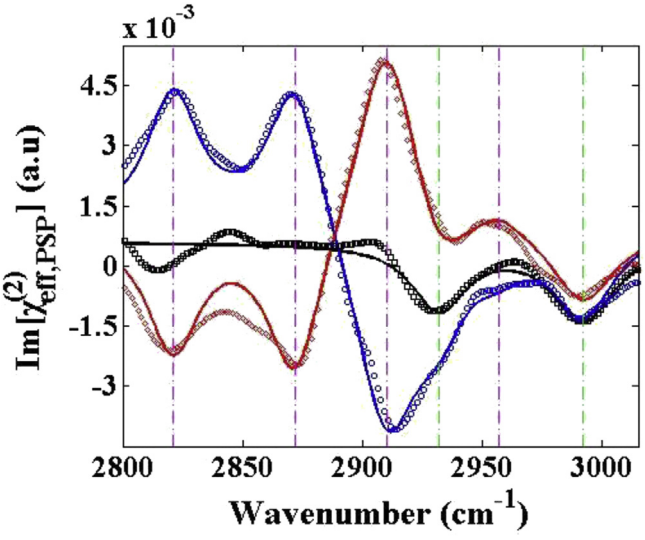

Figure 2. The Im ($\chi^{(2)}$) spectra of the carvone air/liquid interfaces with PSP polarization combination: S-carvone (blue), R-carvone (red), racemic mixture (black). Dots are the original sample data, and lines are the fitting curves.

Table 1. The fitting dates of the chiral SFG spectra of S-, R- and the racemic mixture of carvone in Figure 2.

q	ω_q (cm^{-1})	Γ_q (cm^{-1})	A_S	A_R	A_{RS}
chiral	2821 ± 1	13.5 ± 0.5	0.59	-0.54	NA
chiral	2873 ± 1	14.5 ± 1.5	0.82	-0.83	NA
chiral	2910 ± 2	16.5 ± 0.5	-1.40	1.43	NA
achiral	2932 ± 1	14.0 ± 0.5	-0.33	-0.32	-0.32
chiral	2957 ± 1	12.5 ± 0.5	-0.09	0.08	NA
achiral	2992 ± 1	16.0 ± 2	-0.54	-0.47	-0.49

The imaging symmetry of the chiral spectra of S- and R-carvone are also destroyed by the obviously achiral spectral feature. Two clear vibrational peaks at 2932 cm^{-1} and 2992 cm^{-1}, labelled with green vertical dashed lines in Figure 2, have negative sign for both S- and R-carvone enantiomers, while these peaks in the racemic mixture spectrum are still remained. Especially for the interference of the negative achiral vibrational peak at 2932 cm^{-1}, the negative chiral vibrational peak at 2910 cm^{-1} of S-carvone has a broad shoulder, while the positive chiral vibrational peak at 2910 cm^{-1} of R-carvone becomes sharper. Though we have carefully calibrated the polarization combination of the HD-SFG, it is stills possible that the achiral signal may come from the "leaking" signal with SSP or PPP polarization combination. The other origin of the achiral signal in the chiral spectra may come from the prochirality at interfaces, which has been detailed discussed by Wang's group [12].

4. Conclusions

In conclusion, we have successfully applied HD-SFG to distinguish the carvone enantiomers at interface without the electronic resonance. In the chiral PSP Im ($\chi^{(2)}$) spectra, the chiral spectral feature can be clearly separated from the achiral spectral feature with the help of the phase sensitivity of HD-SFG.

Declarations

Author contribution statement

Yang Wang: Performed the experiments; Analyzed and interpreted the data; Wrote the paper.

Jianbin Du: Performed the experiments.

Xiangyun Ma: Performed the experiments; Analyzed and interpreted the data.

Huijie Wang: Analyzed and interpreted the data.

Keng Chou, Qifeng Li: Conceived and designed the experiments.

Funding statement

This work was supported by the National Key Research and Development Program of China (2017YFC0803600).

Competing interest statement

The authors declare no conflict of interest.

Additional information

No additional information is available for this paper.

References

[1] B.W.T. Kelvin, The Molecular Tactics of a Crystal, 2012.
[2] P.K. Johansson, L. Schmuser, D.G. Castner, Nonlinear optical methods for characterization of molecular structure and surface chemistry, Top. Catal. 61 (Jun 2018) 1101–1124.
[3] L.D. Barron, Molecular Light Scattering and Optical Activity, Cambridge University Press, 2004.
[4] E. Charney, E. Charney, The Molecular Basis of Optical Activity: Optical Rotatory Dispersion and Circular Dichroism, Wiley, New York, 1979.
[5] N. Berova, K. Nakanishi, R.W. Woody, Circular Dichroism: Principles and Applications, 912, Wiley-VCH, New York, 2000.
[6] J.D. Byers, H.I. Yee, T. Petralli-Mallow, J.M. Hicks, Second-harmonic generation circular-dichroism spectroscopy from chiral monolayers, Phys. Rev. B Condens. Matter 49 (May 15 1994) 14643–14647.
[7] M.A. Belkin, Y.R. Shen, Doubly resonant IR-UV sum-frequency vibrational spectroscopy on molecular chirality, Phys. Rev. Lett. 91 (Nov 21 2003) 213907.
[8] M.A. Belkin, T.A. Kulakov, K.H. Ernst, L. Yan, Y.R. Shen, Sum-frequency vibrational spectroscopy on chiral liquids: a novel technique to probe molecular chirality, Phys. Rev. Lett. 85 (Nov 20 2000) 4474–4477.
[9] M.A. Belkin, T.A. Kulakov, K.H. Ernst, S.H. Han, Y.R. Shen, Resonant sum-frequency generation in chiral liquids, Opt. Mater. 21 (Jan 2003) 1–5.
[10] J. Wang, X.Y. Chen, M.L. Clarke, Z. Chen, Detection of chiral sum frequency generation vibrational spectra of proteins and peptides at interfaces in situ, Proc. Natl. Acad. Sci. U. S. A 102 (Apr 5 2005) 4978–4983.
[11] L. Fu, J. Liu, E.C.Y. Yan, Chiral sum frequency generation spectroscopy for characterizing protein secondary structures at interfaces, J. Am. Chem. Soc. 133 (2011) 8094–8097.
[12] L. Fu, Y. Zhang, Z.H. Wei, H.F. Wang, Intrinsic chirality and prochirality at Air/R-(+)- and S-(-)-limonene interfaces: spectral signatures with interference chiral sum-frequency generation vibrational spectroscopy, Chirality 26 (Sep 2014) 509–520.
[13] M. Okuno, T.A. Ishibashi, Chirality discriminated by heterodyne-detected vibrational sum frequency generation, J. Phys. Chem. Lett. 5 (Aug 21 2014) 2874–2878.
[14] S. Lotze, J. Versluis, L.L. Olijve, L. van Schijndel, L.G. Milroy, I.K. Voets, et al., Communication: Probing the absolute configuration of chiral molecules at aqueous interfaces, J. Chem. Phys. 143 (Nov 28 2015) 201101.
[15] M.L. McDermott, P.B. Petersen, Robust self-referencing method for chiral sum frequency generation spectroscopy, J. Phys. Chem. B 119 (Sep 24 2015) 12417–12423.
[16] M. Okuno, T.A. Ishibashi, Sensitive and quantitative probe of molecular chirality with heterodyne-detected doubly resonant sum frequency generation spectroscopy, Anal. Chem. 87 (Oct 6 2015) 10103–10108.
[17] H.-F. Wang, Sum frequency generation vibrational spectroscopy (SFG-VS) for complex molecular surfaces and interfaces: spectral lineshape measurement and analysis plus some controversial issues, Prog. Surf. Sci. 91 (Dec 2016) 155–182.
[18] L. Schmuser, S. Roeters, H. Lutz, S. Woutersen, M. Bonn, T. Weidner, Determination of absolute orientation of protein alpha-helices at interfaces using phase-resolved sum frequency generation spectroscopy, J. Phys. Chem. Lett. 8 (Jul 6 2017) 3101–3105.
[19] L. Fu, G. Ma, E.C.Y. Yan, In situ misfolding of human islet amyloid polypeptide at interfaces probed by vibrational sum frequency generation, J. Am. Chem. Soc. 132 (Apr 21 2010) 5405–5412.
[20] K.T. Nguyen, An electronically enhanced chiral sum frequency generation vibrational spectroscopy study of lipid-bound cytochrome c, Chem. Commun. 51 (2015) 195–197.
[21] K. Meister, S. Lotze, L.L.C. Olijve, A.L. DeVries, J.G. Duman, I.K. Voets, et al., Investigation of the ice-binding site of an insect antifreeze protein using sum-frequency generation spectroscopy, J. Phys. Chem. Lett. 6 (Apr 2 2015) 1162–1167.
[22] N. Ji, V. Ostroverkhov, C.-Y. Chen, Y.-R. Shen, Phase-sensitive sum-frequency vibrational spectroscopy and its application to studies of interfacial alkyl chains, J. Am. Chem. Soc. 129 (Aug 22 2007) 10056–+.
[23] I.V. Stiopkin, H.D. Jayathilake, A.N. Bordenyuk, A.V. Benderskii, Heterodyne-detected vibrational sum frequency generation spectroscopy, J. Am. Chem. Soc. 130 (Feb 20 2008) 2271–2275.
[24] S. Yamaguchi, T. Tahara, Heterodyne-detected electronic sum frequency generation: "Up" versus "down" alignment of interfacial molecules, J. Chem. Phys. 129 (Sep 14 2008).
[25] V.M. Dembitsky, Astonishing diversity of natural surfactants: 7. Biologically active hemi- and monoterpenoid glycosides, Lipids 41 (Jan 2006) 1–27.
[26] A. Wei, T. Shibamoto, Antioxidant activities and volatile constituents of various essential oils, J. Agric. Food Chem. 55 (Mar 7 2007) 1737–1742.
[27] I.S. Martinez, M.D. Peterson, C.J. Ebben, P.L. Hayes, P. Artaxo, S.T. Martin, et al., On molecular chirality within naturally occurring secondary organic aerosol particles from the central Amazon Basin, Phys. Chem. Chem. Phys. 13 (2011) 12114–12122.
[28] D. Hu, Z. Yang, K.C. Chou, Interactions of polyelectrolytes with water and ions at air/water interfaces studied by phase-sensitive sum frequency generation vibrational spectroscopy, J. Phys. Chem. C 117 (2013) 15698–15703.
[29] T.J. Leitereg, D.G. Guadagni, J. Harris, et al., Chemical and sensory data supporting the difference between the odors of the enantiomeric carvones, J. Agric. Food Chem. 19 (1971) 785–787.
[30] L. Matthias, L. Anne, T. Peter, Enantioselectivity of odor perception in squirrel monkeys and humans, Am. J. Physiol. Regul. Integr. Comp. Physiol. 277 (1999) R1098–R1103.
[31] D. Hu, K.C. Chou, Re-evaluating the surface tension analysis of polyelectrolyte-surfactant mixtures using phase-sensitive sum frequency generation spectroscopy, J. Am. Chem. Soc. 136 (2014) 15114–15117.
[32] R.E. Pool, J. Versluis, E.H. Backus, M. Bonn, Comparative study of direct and phase-specific vibrational sum-frequency generation spectroscopy: advantages and limitations, J. Phys. Chem. B 115 (Dec 29 2011) 15362–15369.

[33] M.T. Dohm, A.M. Potscavage, R.F. Niedziela, Infrared optical constants for carvone from the mie inversion of aerosol extinction spectra, J. Phys. Chem. A 108 (Jun 24 2004) 5365–5376.

[34] H.F. Wang, W. Gan, R. Lu, Y. Rao, B.H. Wu, Quantitative spectral and orientational analysis in surface sum frequency generation vibrational spectroscopy (SFG-VS), Int. Rev. Phys. Chem. 24 (Apr 2005) 191–256.

[35] R.H. Zheng, W.M. Wei, M. Xu, Q. Shi, Sum-frequency vibrational spectroscopy of limonene chiral liquids due to the nonadiabatic effect, Phys. Chem. Chem. Phys. 20 (Mar 7 2018) 7053–7058.